SPARSITY-BASED THRESHOLDING CRITERION FOR SPURIOUS ECHO REMOVAL AND DENOISING MAGNETIC RESONANCE SPECTRA USING RATIONAL-DILATION WAVELET TRANSFORM**

Ch. Sagar [1*], D. Kumar Singh [2], N. Sharma [1]

[1] School of Biomedical Engineering at Indian Institute of Technology (BHU), Varanasi, Uttar Pradesh, India; e-mail: chiranjeevs.rs.bme16@itbhu.ac.in, deepakbhu@gmail.com, neeraj.bme@itbhu.ac.in
[2] Department of Oncology, Apex Super-Speciality Hospital and Post Graduate Institute, Varanasi, Uttar Pradesh, India

Biological signals such as magnetic resonance spectroscopy (MRS) signals are susceptible to noise and artifacts. The information obtained from these signals is significant in analyzing human physiological conditions. MRS, a non-ionizing and non-invasive method, presents an effective alternative method to biopsy for diagnosis and analysis from generated signals that are rich in chemical information of the tissues in the region of interest. A persisting problem of this method is the presence of noise and artifacts causing misinterpretation and subsequent incorrect diagnosis. The present research proposes a denoising strategy using the rational-dilation wavelet transform-based signal decomposition and a thresholding criterion designed using the L_{pq}-norm-based sparsity measure of the decomposition levels of the signal. Compared with the standard state-of-the-art methods, which are effective in denoising but can cause distortion of the signal at discontinuities, the proposed method can remove artifacts such as spurious echoes present in the magnetic resonance signals and improve the signal-to-noise ratio without distorting the signal.

Keywords: *magnetic resonance spectroscopy, rational-dilation, sparsity, L_{pq}-norm, spurious echo.*

КРИТЕРИЙ ПОРОГОВОЙ ОБРАБОТКИ НА ОСНОВЕ РАЗРЕЖЕННОСТИ ДЛЯ УДАЛЕНИЯ ПАРАЗИТНОГО ЭХА И ШУМОПОДАВЛЕНИЯ МАГНИТНО-РЕЗОНАНСНЫХ СПЕКТРОВ С ИСПОЛЬЗОВАНИЕМ РАСШИРЕННОГО ВЕЙВЛЕТ-ПРЕОБРАЗОВАНИЯ

Ch. Sagar [1*], D. Kumar Singh [2], N. Sharma [1]

УДК 543.422.23

[1] Школа биомедицинской инженерии Индийского технологического института (BHU), Варанаси, Уттар-Прадеш, Индия; e-mail: chiranjeevs.rs.bme16@itbhu.ac.in, deepakbhu@gmail.com, neeraj.bme@itbhu.ac.in
[2] Специализированная больница Apex и Институт последипломного образования, Варанаси, Уттар-Прадеш, Индия

(Поступила 25 марта 2021)

Предложена стратегия шумоподавления с использованием разложения сигнала на основе расширенного вейвлет-преобразования и критерия пороговых значений, разработанного с использованием меры разреженности на основе L_{pq}-нормы уровней разложения сигнала. По сравнению со стандартными современными методами, которые эффективны при шумоподавлении, но могут вызывать искажение сигнала при нарушениях непрерывности, предлагаемый метод может удалить артефакты, например ложные эхо-сигналы, и улучшить отношение сигнал/шум без искажения сигнала.

Ключевые слова: *магнитно-резонансная спектроскопия, рациональное расширение, разреженность, L_{pq}-норма, ложное эхо.*

**Full text is published in JAS V. 89, No. 3 (http://springer.com/journal/10812) and in electronic version of ZhPS V. 89, No. 3 (http://www.elibrary.ru/title_about.asp?id=7318; sales@elibrary.ru).

Introduction. Magnetic resonance spectroscopy (MRS) is a promising non-invasive and non-ionizing methodology of studying and quantifying the biochemical information of tissue metabolites from the anatomical region of interest [1]. This method can aid in early diagnosis of different types of cancer pathology, study treatment progression, or therapy. Because of these attributes, this valuable tool is also sometimes referred to as "virtual biopsy" [2]. An *in vivo* MR spectrum in the time domain can be expressed as

$$y(t) = \sum_{k=1}^{K} a_k e^{(j\phi_k)} e^{(-d_k t + 2\pi f_k t)} + B(t) + w(t) + \varepsilon(t) \ , \quad (1)$$

where K is the number of metabolites, a_k is the amplitude, ϕ_k signifies the phase shift, d_k symbolizes the damping correction, and f_k designates the frequency shifts due to the field heterogeneity of the k^{th} metabolite; $B(t)$ denotes the baseline due to macromolecules/lipid contamination, $w(t)$ marks the water resonance, and $\varepsilon(t)$ is the white noise with standard deviation σ.

Magnetic resonance spectroscopy finds its application in both research and clinical setup, and an increasing number of research publications in the last two decades ensure its near acceptance as an important clinical diagnostic tool. Post-acquisition of signals, the standard workflow of an *in vivo* MRS study, follows three steps: pre-processing, spectral analysis, and quantitation. Pre-processing of an acquired MR spectrum is fundamental for precise analysis and subsequent quantitation of the metabolites concerned, as, along with the chemical information, a significant amount of irrelevant information such as noise, spikes, and spurious echoes are also present.

The presence of noise and signal contamination (especially spurious echoes or spikes) due to internal systems or external environmental sources are inherent in any signal acquisition system. Overlapping of echoes over metabolite peaks poses a serious challenge in the accurate quantification of the metabolite information [3]. Therefore, denoising remains a prerequisite and is essential to every signal processing and analysis method. The basic objective of denoising is to improve the qualitative as well as the quantitative information for a reliable and accurate analysis of a signal spectrum by reducing the effect of noise and artifacts.

Previously, traditional denoising methods have used either time domain or frequency domain-based analysis. A Fourier transform and its variants have been used as global transformation functions for signal analysis, but are regarded as inadequate in many cases related to singularities or nonstationary signals. The short-time Fourier transform method, incorporating the short-term window function, does not meet the requirements either. The introduction of a wavelet transform (WT) as an alternative has opened up a new paradigm in the field of signal processing. The seminal works of Daubechies [4] in filter design and that of Mallat [5] in the development of efficient algorithms for discrete WTs created a platform for the current advances in wavelet-based signal processing [6].

The introduction of wavelets has significantly helped in resolving the problems associated with the nonstationary signals. WT provides a multiresolution, time–frequency scale analysis and it is capable of dealing with the breakdown points and discontinuities in the higher derivatives. Similar to traditional high-pass and low-pass filtering, WT decomposes a signal into 'detail' and 'approximation' coefficient levels. A significant feature of WT is the dimension reduction of the given datapoints using orthogonal bases and hence, presenting a sparse representation of data. Sparsity in decomposed wavelet coefficients of a signal can be exploited for denoising by applying an appropriate thresholding method [7]. As most of the real biological signals have high redundancy, wavelet analysis using sparsity as an index of threshold determination can be utilized as a denoising methodology for signals.

Theory. *Rational-dilation wavelet transform (RADWT).* This WT belongs to a family of over-complete, rational dilation-based (i.e., nondyadic) transforms [8]. Unlike most of the existing over-complete WTs, where over-completeness is attained only by increasing the temporal sampling in frequency bands, overcomplete RADWTs increase sampling both in time and frequency bands providing different redundancy factors and better resolution of the signal. The implementation of this transform is based on a fast Fourier transform-based filter bank that provides greater design flexibilities and can be utilized to generate several wavelet attributes, which is difficult to realize with far infrared radiation filter-bank-based transforms. An array of Q-factors, frequency resolution, and redundancy factors are achievable with this family of WT. The iterated filter bank for RADWTs is realized as depicted in Fig. 1a, whereas the analysis and synthesis parts of the filter bank for the family of RADWT are represented in Fig. 1b.

The redundancy factor of the WT is calculated as

$$\mathrm{Red}(p,q,s) = \frac{1}{s}\frac{1}{1-(p/q)} . \quad (2)$$

For $p = 7$, $q = 8$, and $s = 3$, the dilation factor is $8/7 \approx 1.14$ and redundancy (Red(p,q,s)) is $8/3 \approx 2.67$. Using these parameters, the wavelet generated resembles a Gabor function and approximates a Gaussian-like shape (a cosine function multiplied with a Gaussian function), which is similar to the MRS signal line shape. It is optimally localized in the time–frequency plane and has a high Q-factor with no ringing effects, as shown in Fig. 2.

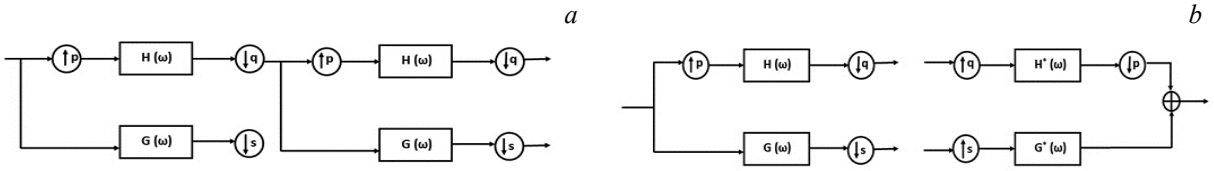

Fig. 1. (a) Iterated filter-bank for RADWT; (b) analysis and synthesis part of the filter-bank, where $H(\omega)$ and $G(\omega)$ are the low-pass and high-pass filters respectively, satisfying perfect reconstruction conditions; p, q, and s are the constant positive integers and the dilation factor is represented as q/p, a rational number.

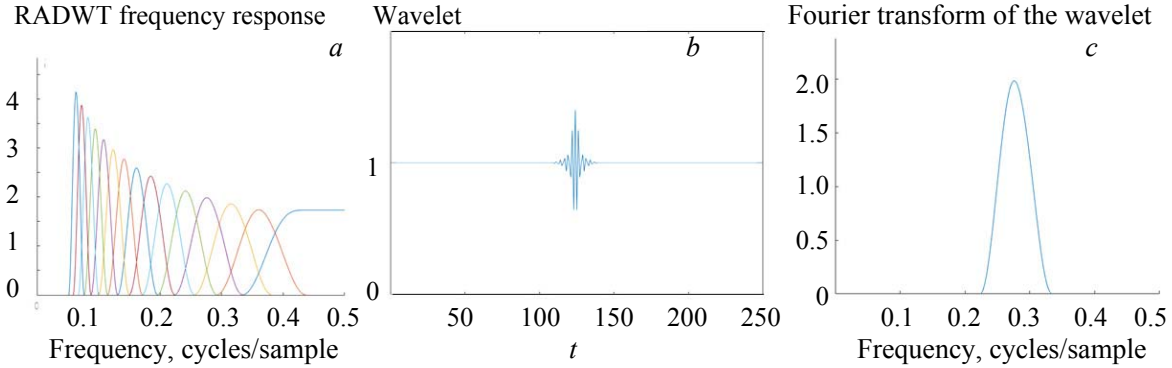

Fig. 2. (a) RADWT frequency response of each of 15 levels of decomposition, $p = 7$, $q = 8$, $s = 15$ levels; (b) wavelet function resembling the 'Gabor' function; (c) Fourier transform of the wavelet function having Gaussian-like shape.

The performance of the above-mentioned overcomplete transform is investigated for denoising of the MR spectroscopy signals. This family of WTs, designed for the discrete-time data, is a slightly overcomplete rational dilation-based (so nondyadic), near shift-invariant and is self-inverting (tight-frame). For the compound MR spectra of individual metabolites with different relaxation times, this family of the tight frame WTs is expected to perform better, as it gives the flexibility to vary frequency resolution and Q-factor, as required.

Sparsity measures ($L_{p,q}$-norm). Among different measures to calculate sparsity, norm-based measures have interesting benefits. $L_{p,q}$-norm is a generalized form of a matrix norm expressed as

$$L_{pq} = \left(\sum_{j=1}^{n} \left(\sum_{i=1}^{m} \left(\left| a_{ij} \right|^{p} \right) \right)^{q/p} \right)^{1/q} . \tag{3}$$

For a vector of n data points, $A = (a_1, ..., a_n)$, the matrix form is represented as $A = (a_{ij})$ such that $i = 1, ..., m$ denotes summation over spatial dimension and $j = 1, ..., n$ denotes the summation of data points. For $p = 2$, $q = 1$, $L_{2,1}$-norm is given as [9]:

$$L_{2,1} = \sum_{j=1}^{n} \left(\sum_{i=1}^{m} \left(\left| a_{ij} \right|^{2} \right) \right)^{1/2} . \tag{4}$$

Here, the spatial domain attributes are measured in L_2 and data points summation is done over L_1-space. $L_{2,1}$-norm, which behaves as an error function, is robust and is used in sparse coding where L_1 norm can be used to enforce sparsity as a penalty term on model parameters. In the current study, a modified form of $L_{2,1}$-norm is used, which is expressed as [10]:

$$L_{2,1} = A_j = \frac{\left(\sum_{i=1}^{n}\left(\left|a_{ji}\right|^2\right)\right)^{1/2}}{\sum_{i=1}^{n}\left|a_{ji}\right|} \quad (5)$$

to calculate the sparsity of each wavelet decomposition level j.

Before wavelet decomposition of MR spectra into different levels, it is necessary to perform some specific pre-processing steps, to prepare it for further analysis.

1. Frequency alignment: free induction decay (FID) is transformed into a frequency domain, and N-acetyl aspartate (NAA) singlet peak (located at 2.01 ppm) has been used as a reference to shift the overall spectra [11, 12].

2. Phase correction: to improve frequency-domain spectral analysis and quantitation, zero-phased correction is required. This correction is performed by multiplying a complex phase factor from the initial points of FID with the complete complex spectrum [13, 14].

3. Eddy current correction (ECC): owing to switching of the magnetic field gradient, eddy currents are produced according to Faraday's law of induction. During signal acquisition, a water-unsuppressed signal along with a water-suppressed signal is acquired following the same protocol. The correction is performed using the Klose method [15] by dividing the phase of the unsuppressed signal from the water-suppressed signal pointwise.

4. Residual water peak suppression: during acquisition, signals are collected using CHESS or a similar sequence in an acquisition protocol to suppress the water resonance, which is usually from 10^3 to 10^4 times larger than the study-related metabolites. Despite suppression, there remains a residual water peak comparable with metabolite peaks in the signal. The Hankel singular value decomposition (HSVD) method has been used to remove these residual water peaks from the signal [16, 17].

Frequency alignment, phase correction, and residual water correction were performed using the jMRUI software platform [18] and ECC was performed on MATLAB.

Wavelet-based denoising is based on the idea of thresholding the decomposed levels obtained by transforming the original data using appropriate wavelets that would resemble the actual signal to obtain better noise separation. For the present study, the chosen wavelet resembles the Gabor function by manipulating the RADWT filter bank parameters, as explained above.

The criteria of the sparsity measure to select the decomposition level have been chosen to be less than 0.1 of the level.

The process of denoising is implemented in the following way: signal acquisition from the MR scanner; performing frequency alignment, phase correction, ECC, and residual water removal; addition of the noise to the signal; decomposition of the signal using RADWT into detailed and approximation levels; as decomposition levels have both positive and negative coefficients and contribute equally to noise and signal, the maximum of each positive and negative set of coefficients are obtained; thresholding criteria are applied to the coefficients and a hard thresholding operation is used to delineate the signal coefficients from the noise coefficients; reconstruction is performed using inverse RADWT using the thresholded coefficients.

Thresholding criteria. Existing methods. The decision of an accurate threshold is important to signal denoising. For values too small, there will be a considerable amount of noise remaining in the signal, and for values too large, some signal features might also get removed. Thresholding a wavelet coefficient for denoising was first proposed by Donohue [19] who used a fixed noise threshold for the decomposition levels. Also, the termed universal threshold is calculated as

$$\lambda = \sigma\sqrt{2\ln N}\,, \quad (6)$$

where N is the signal length or decomposition level length and σ is the standard deviation of the noise given by [20]:

$$\sigma = \text{median}\,|Y_{ij}|\,/0.6745. \quad (7)$$

Stein's unbiased risk estimate (SURE) threshold and the minimax threshold [21] are two of the most widely used and better performing fixed threshold estimates. Based on wavelet shrinkage [17, 22–27], wavelet coefficient modeling [28] and modulus maxima [29] many denoising methods have been developed with performances better than the conventional filtering operation [30]. Further, considering different properties of wavelet decomposition coefficients, different approaches of thresholding criteria have been proposed [31–35]. The idea of adaptive thresholding [22, 36] has evolved from the limitations of fixed thresholding methods such as a) same noise threshold for each coefficient of a decomposition level without considering its bias and

b) inability to discriminate between the coefficients when magnitudes of signal and noise coefficients are close. The above-mentioned issues are practically visible when analyzing a real experimental signal. Srivastava et al. [37] proposed a denoising method for adaptive noise threshold selection depending on the decomposition levels selected with the application on cw-ESR spectra and presented promising results.

Proposed criteria. MR spectra are the combination of different chemical metabolite profiles of tissues resonating at frequencies slightly different from one another based on their local environments. The spectrum obtained is complex and the presence of noise and spurious echoes make denoising a challenging task. The method proposed by Srivastava et al. is promising but is limited in maintaining individual peak morphology given the nature of MR spectra, which show considerable differences in individual peak characteristics.

In the present work, an adaptive thresholding criterion is proposed where RADWT and $L_{p,q}$-norm sparsity measure are employed to determine the decomposition levels and the threshold calculation for each decomposition level. The proposed method is implemented in the following way:

1. The signal is decomposed into detailed and approximation levels.

2. Sparsity measure, A of each detailed coefficient level is calculated and for a level having $A > 0.1$, the decomposition level is selected up to which the wavelet decomposition and subsequently, level thresholding, are performed.

3. To cover all the positive and negative coefficients of the decomposition level, $\max|w_j > 0|$ and $\max|w_j < 0|$ are obtained.

4. On each subset for a decomposition level, the thresholding criteria are applied as

$$\lambda_{j,L} = M_j - \alpha_{j,L}(M_j - \max|w_j < 0|),\ \lambda_{j,H} = M_j + \alpha_{j,H}(M_j - \max|w_j > 0|). \quad (8)$$

5. Hard thresholding function is applied to remove noisy coefficients from the signal components.

6. Using these coefficients, inverse RADWT is performed to reconstruct the denoised signal.

Here $\lambda_{j,L}$ and $\lambda_{j,H}$ represent thresholds for negative and positive coefficients at the decomposition level j respectively. M_j is the median and w_j is the wavelet coefficient of the decomposition level j. In the present work, the median of the coefficients is considered, as it gives a better representation of the data when there is a possibility of a small proportion of extremely large or small value in the data, being the most resistant statistic. The presence of spikes or echoes is expected to generate wavelet coefficients of such a nature. α_j is the level-dependent parameter for adjusting threshold values and is defined as

$$\alpha_j = (1 - A_j/A_r), \quad (9)$$

where the reference sparsity level $A_r = (A_j + A_{j+1})/2$.

Thresholding function. In the proposed method, a hard thresholding function was used on the noise thresholded coefficients for the accurate separation of the noise from the signal coefficients. Combining the hard thresholding with the proposed thresholding criterion, the function is implemented as

$$\tilde{w}_{j,i} = \begin{cases} 0: \ \lambda_{j,L} \le w_{j,i} \le \lambda_{j,H}, \\ w_{j,i}: \ \text{ohterwise}, \end{cases} \quad (10)$$

where $\tilde{w}_{j,i}$ is the noise thresholded wavelet coefficient at the decomposition level j.

Method. The eventual goal of denoising a medical signal is to obtain a better feature representation for the accurate quantitation and subsequent classification for diagnostic purposes. The use of the WT-based thresholding approaches for denoising is not new and different thresholding criteria have been presented in scientific literature since Donoho et al. [19]. MR spectra generate complex-valued data with artifacts of varying characteristics depending upon the internal MR system as well as external environmental factors. The existing approaches are relatively efficient and sometimes aggressive in reducing the noise, causing distortions in the shape and envelope of the original MR spectra. The novel approach presented in this paper utilizes the flexibility of RADWT filters for better sparse representation of the signal and $L_{p,q}$-norm-based index to capture the sparsity for effective thresholding to reduce the noise while maintaining the structure of the original signal. This is important for accurate feature-based studies and analysis and can also be used as inputs to machine-learning classifiers for further analysis and inferences subjected to diagnostic purposes.

Dataset used. *MRS.* All MR signals acquired are water-suppressed FID ^{1}H single-voxel spectroscopy signals of the human brain at a magnetic field strength of 1.5 T Magnetom Avanto (Version BV-I7A; Siemens Medical System, Erlangen, Germany) with PRESS pulse sequence, at echo time TE = 35 ms and repetition time TR = 1500 ms. The number of data points in the FID is 1024. A total of 249 signals (38 with tu-

mor, 211 normal) has been obtained. The dataset used for this study is retrospective; hence, the requirement of patient's consent was waived by the Institute Ethical Committee. Eight signals were discarded on the grounds of corruption of the prominent peaks in the signal because of the artifacts due to patient movements. A water-unsuppressed FID with a similar protocol is also acquired for the eddy current correction.

To examine the range of application of the proposed method, the present method is also applied to the signals acquired from the Raman spectroscopy data bank.

Evaluation metrics. To compare the level of noise present in a signal, a signal-to-noise ratio is used. It is calculated by taking the ratio of summed squared magnitude of the signal and the noise:

$$\mathrm{SNR} = \frac{\sum_{i=1}^{N} (x_i)^2}{\sum_{i=1}^{N} (x_i - \tilde{x})^2}. \tag{11}$$

Root mean-square-error is a measure to show the amount of deviation of the residual error between the original and the reconstructed signal. It is calculated as

$$\mathrm{RMSE} = \sqrt{\frac{\sum_{i=1}^{N} (x_i - \tilde{x})^2}{N}}, \tag{12}$$

where x_i is the original signal and $\tilde{x}$ is the reconstructed signal after denoising.

Structural similarity index [38] is an objective measure commonly used in comparing the structural quality of images before and after processing in signals. The reconstructed signal can be compared with the original signal for structural similarity. In this study, the focus is maintained on the spurious echo removal along with the overall denoising of the signal, and therefore, SSIM was expected to be within the range 0.85 to 0.95. It is calculated as

$$\mathrm{SSIM}(X,Y) = \frac{(2\mu_X\mu_Y + c_1)(2\sigma_{XY} + c_2)}{(\mu_X^2 + \mu_Y^2 + c_1)(\sigma_X^2 + \sigma_Y^2 + c_2)}. \tag{13}$$

Here the denoised signal is represented as X and the original signal as the reference signal Y; μ_X and μ_Y are the mean and σ_X and σ_Y are the standard deviation of X and Y respectively; σ_{XY} is the covariance of X and Y; c_1 and c_2 are stabilizing constant terms, each for mean and standard deviation.

MR spectra contain peaks specific to metabolites present in the tissues under study. The position of peaks and their amplitudes are essentially the most important feature for accurate quantification of metabolites and subsequent diagnosis. The operation of the thresholding on the signal wavelet coefficients can alter the peak amplitudes when reconstructed. Therefore, the peak amplitude of a specific metabolite at its position before and after the denoising operation has been measured to test the perfect reconstruction of the present method. NAA peak at 2.01 ppm, Cr peak at 3.01 ppm, and Cho peak at 3.21 ppm are taken as reference peaks to compare the measurements.

Experiments. In the first study, RADWT decomposition and the thresholding with different criteria, existing as well as proposed, were applied on MRS signals to evaluate the peak amplitude variations on the dataset of 249 MRS signals. Table 1 shows the mean values of the normalized amplitudes of NAA, Cr, and Cho peaks after denoising. In the second study, different thresholding methods were applied to MR signals containing spurious echoes near a peak to evaluate their ability to remove spurious echoes. Wavelet scattering transform was used on each of the denoised signals to obtain a scattergram coefficient matrix to compare the elimination of the spurious echoes from the signal. Scalograms plotting was done for the visualization of the echo component from the signal. Figures 3a–d clearly show that the present method can remove the echo component more effectively than the other methods. In the third study, the efficiency of the proposed method in overall denoising of the signal was evaluated (i) without adding any additional noise to the signal, and then (ii) by adding additive white Gaussian noise to obtain noisy signals of 10, 20, 30, and 50 dB. The parameter indices calculated for the comparison were SNR, RMSE, and SSIM. As the proposed method is based on an overcomplete rational-dilation-based WT, which is nondyadic, denoising one using double density dual-tree DWT (DDDT-DWT) [39, 40], a dyadic transform method has been performed for comparison. A thresholding method proposed by Srivastava et al. [37] was also implemented for denoising. Finally, five test Raman signals were selected and the denoising was performed by adding the additive white Gaussian noise of 25 dB to evaluate the efficacy of the proposed method for the different experimental or biological signals.

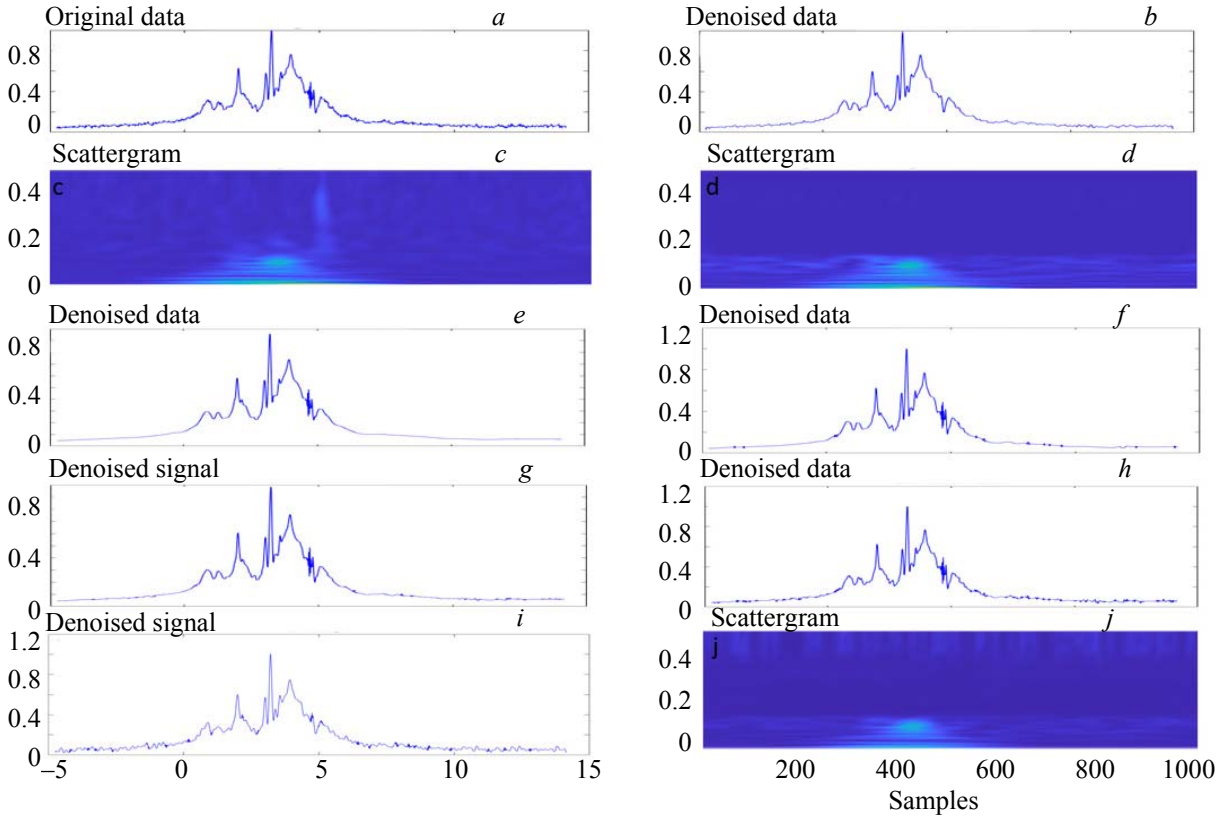

Fig. 3. Visualization of spurious echo removal for comparison of different existing approaches: (a) Original signal with spurious echo, spurious echo removal plot using different methods; (b) proposed method signal plot; (c) and (d) scalogram plot of (a) and (b); (e) using minimax-soft thresholding; (f) using minimax-hard thresholding, (g) using SURE-soft thresholding; (h) using SURE hard thresholding; (i) using method [37] signal plot; (j) corresponding scalogram plot.

TABLE 1. Comparison of Peak Amplitudes after Denoising Using Different Thresholds

Method	NAA (2.01 ppm)	Cr (3.02 ppm)	Cho (3.21 ppm)
Before denoising	0.6304	0.5823	1.000
Method [37]	0.5998	0.5708	1.005
Minimax-hard	0.614	0.5703	1.027
Minimax-soft	0.5828	0.5623	0.946
SURE-hard	0.6214	0.5718	1.015
SURE-soft	0.6071	0.5701	0.9838
Proposed	0.6284	0.5799	0.9983

Results and discussion. The assessment of an effective signal denoising method cannot be just limited to the increase in the SNR factor. The abilities to differentiate between the weak signal components, maintaining the peak features such as the amplitude and artifact correction are equally important. Considering the above factors, three different experiments have been designed in the present study. In the first experiment, different thresholding criteria were applied to RADWT decomposition coefficients and the reconstructed signals were compared with the peak amplitudes of NAA, Cr, and Cho. The complete dataset of 219 MR signals was used in this study and each signal was normalized before denoising, by dividing the signal by its maximum amplitude. In the following Table 1, the mean amplitude of 38 signals with the tumor cases has been shown where the Cho peak is used as the normalization peak. Similar results were obtained for the normal case signals where the NAA peak was taken as the normalization peak. From the results obtained from this experiment, it is observed that the reconstruction using the proposed method of denoising is the closest to maintaining the peak amplitude of the signal. In this experiment, seven signals containing spurious

echoes were chosen from the dataset. Spurious echoes result from the local susceptibility variations or insufficient spoiler gradient power during the acquisition. These echoes may overlap the metabolite peaks causing incorrect estimation of peak areas and therefore concentration. On the signals with the spurious echoes embedding the signal, the proposed method of using the Gabor function-like wavelet for decomposition was effective in eliminating the spurious echoes, as shown in Fig. 4. Other methods of thresholding were also tested using DWT with standard thresholds and the thresholding method proposed by Srivastava et al. [37]. To visualize the effectiveness of each method, first-order scattering transform matrix of the denoised signals was calculated, and scalograms were plotted with the signal.

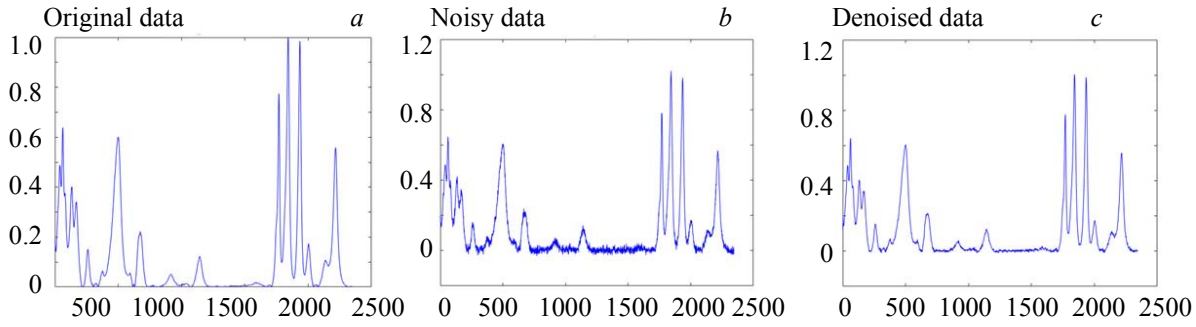

Fig. 4. Denoising of Raman test signal by the proposed method.

From the above comparisons, it can be deduced that although standard state-of-the-art methods render significant denoising effects, there are some morphological issues related to the denoised signals. It is observed in the signal plots that the denoised signals using the standard thresholds led to extra smoothing of the peaks, especially weak signals. Also, none of these methods was able to eliminate spurious echo components from the signal. The method proposed by Srivastava et al. [37] was able to reduce the echo component from the signal but not remove it completely.

From the above two studies, it was concluded that the present method is better at handling artifacts while maintaining the peak amplitudes after the reconstruction of the MR signal. It can therefore be inferred that for the experimental biological signals, which contain discontinuities and the weak signal components, the performance of the discussed method is significantly better. In this study, the denoising efficiency of the proposed method was evaluated by calculating SNR, RMSE, and SSIM. After analyzing the performance of existing methods in the above studies, most of them were eliminated for further assessments. Therefore, for comparison, denoising was performed using the DDDT-DWT method and method proposed in Srivastava et al. [37] only, as they performed better in the previous two studies. For this study, denoising was performed on the complete dataset of 219 signals (seven spurious echoes containing signals as well) and adding additive white Gaussian noise. SNR, RMSE, and SSIM for the noisy signal were 25.5682, 0.00925, and 0.9164 dB, respectively. After denoising using three different methods on 219 signals, the evaluated parameter index values shown in Table 2 are the mean values over all signal outputs.

TABLE 2. Comparison Results of Different Methods for Denoising Efficiency

Method	SNR (dB)	RMSE	SSIM
Noisy signal	25.5682	0.00925	0.9164
DDDT-DWT	26.3170	0.01268	0.8791
Method [37]	27.2768	0.00948	0.9523
Proposed	30.4193	0.00345	0.9604

Similar experiments were also performed after adding the noise of 30, 40, and 50 dB and the results follow a similar pattern. Hence, it is concluded that the present method is efficient in denoising while maintaining the peak features of signals as supported by the parameter indices for evaluation. The calculated standard deviations of these indices for 219 signals are 0.7615, 0.0017, and 0.0181 for SNR, RMSE, and SSIM, respectively, which further implies the stability and specificity of the proposed method for different noisy sig-

nals. The Raman test signals were used to evaluate the application of the proposed method on the other experimental signals. With 25 dB of additive white Gaussian noise added, the SNR, RMSE, and SSIM values obtained were 32.8997, 0.0031, and 0.9684, respectively, after denoising.

Conclusions. With the method proposed in this paper, it is shown that the denoising of signals is effective in terms of gain in SNR values, removal of the unwanted artifacts such as spurious echoes, without distorting the peak characteristics of the spectra. This denoising approach has been designed with the prospects of using the wavelets as feature extractors to be fetched as inputs to neural networks and machine-learning architectures for further MRS study, and the results shown above are promising for further analysis. The flexibility in time–frequency resolution or choice of wavelet function using RADWT helps in sparser feature representation of signal, which can be used as an input to different available classifiers directly to further obtain the most robust and specific analysis. Besides MR spectra, the proposed method has also been applied to Raman spectroscopy signals, showing improved outcomes. Therefore, it can be inferred that other than MRS, the present method also finds its application in denoising different biological or experimental signals.

Acknowledgments. This work is supported by the Indian Institute of Technology (BHU), Varanasi, UP, India.

REFERENCES

1. C. E. Mountford, P. Stanwell, A. Lin, S. Ramadan, B. Ross, *Chem. Rev.*, **110**, No. 5, 3060–3086 (2010), doi: 10.1021/cr900250y.
2. A. Lin, T. Tran, S. Bluml, S. Merugumala, H.-J. Liao, B. Ross, *Sem. Neurol.*, **32**, No. 4, 432–453 (2013), doi: 10.1055/s-0032-1331814.
3. S. P. Kyathanahally, A. Döring, R. Kreis, *Mag. Res. Med.*, **80**, No. 3, 851–863 (2018), doi: 10.1002/mrm.27096.
4. I. Daubechies, *Ten Lectures on Wavelets*, Philadelphia, Pa: Society for Industrial and Applied Mathematics (1992).
5. S. G. Mallat, *IEEE Trans. Acoust., Speech, Signal Proc.*, **37**, No. 12, 2091–2110 (1989), doi: 10.1109/29.45554.
6. F. Ehrentreich, *Anal. Bioanal. Chem.*, **372**, No. 1, 115–121 (2002), doi: 10.1007/s00216-001-1119-4.
7. J. Karvanen, A. Cichocki, *Measuring Sparseness of Noisy Signals*, *4th Int. Symposium Independent Component Analysis and Blind Signal Separation*, 125–130 (2003).
8. I. Bayram, I. W. Selesnick, *IEEE Trans. Signal Process*, **57**, No. 8, 2957–2972 (2009), doi: 10.1109/TSP.2009.2020756.
9. C. Ding, D. Zhou, X. He, H. Zha, *Proc. Int. Conf. Machine Learning – ICML'06*, Pittsburgh, Pennsylvania, 281–288 (2006), doi: 10.1145/1143844.1143880.
10. M. Khosravy, N. Nitta, N. Gupta, N. Patel, N. Babaguchi, *Compressive Sensing in Healthcare*, Elsevier, 43–63 (2020).
11. W. Wu et al., *J. Chem. Inf. Model.*, **46**, No. 2, 863–875 (2006), doi: 10.1021/ci050316w.
12. G. F. Giskeødegård, et al., *Anal. Chim. Acta*, **683**, No. 1, 1–11 (2010), doi: 10.1016/j.aca.2010.09.026.
13. L. Chen, Z. Weng, L. Goh, M. Garland, *J. Mag. Res.*, **158**, No. 1-2, 164–168 (2002), doi: 10.1016/S1090-7807(02)00069-1.
14. F. Jiru, *Europ. J. Radiology*, **67**, No. 2, 202–217 (2008), doi: 10.1016/j.ejrad.2008.03.005.
15. U. Klose, *Mag. Res. Med.*, **14**, No. 1, 26–30 (1990), doi: 10.1002/mrm.1910140104.
16. W. W. F. Pijnappel, A. van den Boogaart, R. de Beer, D. van Ormondt, *J. Mag. Res.*, **97**, No. 1, 122–134 (1992), doi: 10.1016/0022-2364(92)90241-X.
17. T. Laudadio, N. Mastronardi, L. Vanhamme, P. Van Hecke, S. Van Huffel, *J. Mag. Res.*, **157**, No. 2, 292–297 (2002), doi: 10.1006/jmre.2002.2593.
18. D. Stefan, et al., *Meas. Sci. Technol.*, **20**, No. 10, 104035 (2009), doi: 10.1088/0957-0233/20/10/104035.
19. D. L. Donoho, *IEEE Trans. Inform. Theory*, **41**, No. 3, 613–627 (1995), doi: 10.1109/18.382009.
20. I. M. Johnstone, B. W. Silverman, *J. Roy. Statist. Soc. Ser. B (Methodological)*, **59**, No. 2, 319–351 (1997).
21. D. L. Donoho, I. M. Johnstone, *Biometrika*, **81**, 425–455 (1994), doi: 10.1093/biomet/81.3.425.
22. Jun Jiang, Jian Guo, Weihua Fan, Qingwei Chen, *Proc. 8th World Congress on Intelligent Control and Automation*, Jinan, China, Jul. 2010, 2894–2898 (2010), doi: 10.1109/WCICA.2010.5554856.

23. G. Y. Chen, T. D. Bui, *IEEE Signal Proc. Lett.*, **10**, No. 7, 211–214 (2003), doi: 10.1109/LSP.2003.811586.
24. R. Hussein, K. B. Shaban, A. H. El-Hag, *Int. Conf. Communications, Signal Processing, and their Applications (ICCSPA'15)*, Sharjah, United Arab Emirates, 1–5 (2015), doi: 10.1109/ICCSPA.2015.7081289.
25. C. Huimin, Z. Ruimei, H. Yanli, *Phys. Proc.*, **33**, 1354–1359 (2012), doi: 10.1016/j.phpro.2012.05.222.
26. Y. Ding, I. W. Selesnick, *IEEE Signal Proc. Lett.*, **22**, No. 9, 1364–1368 (2015), doi: 10.1109/LSP.2015.2406314.
27. G. Chen, W. Xie, Y. Zhao, *Fourth Int. Conf. Intelligent Control and Inform. Proc. (ICICIP)*, Beijing, China, Jun. 2013, 570–574 (2013), doi: 10.1109/ICICIP.2013.6568140.
28. L. Sendur, I. W. Selesnick, *IEEE Trans. Signal Proc.*, **50**, No. 11, 2744–2756 (2002), doi: 10.1109/TSP.2002.804091.
29. Y. Liu, X. Cheng, *Fourth Int. Conf. Fuzzy Systems and Knowledge Discovery (FSKD 2007)*, Haikou, China, 32–35 (2007), doi: 10.1109/FSKD.2007.90.
30. I. K. Fodor, *J. Electron. Imaging*, **12**, No. 1, 151 (2003), doi: 10.1117/1.1525793.
31. C. He, J. Xing, J. Li, Q. Yang, R. Wang, *Math. Prob. Eng.*, **2015**, 1–9 (2015), doi: 10.1155/2015/280251.
32. T. Hui, C. Lin, L. Zengli, C. Zaiyu, *Wavelet Image Denoising Based on the New Threshold Function*, **4** (2013).
33. S. Jangjit, M. Ketcham, *Engineering J.*, **21**, No. 7, 141–155 (2017), doi: 10.4186/ej.2017.21.7.141.
34. L. Jing-yi, L. Hong, Y. Dong, Z. Yan-sheng, *Math. Prob. Eng.*, **2016**, 1–8 (2016), doi: 10.1155/2016/3195492.
35. S. A. A. Karim, M. T. Ismail, M. K. Hasan, J. Sulaiman, H. Sakidin, *Denoising Using New Thresholding Method*, Johor Bahru, Malaysia, 0300342 (2016), doi: 10.1063/1.4954570.
36. S. G. Chang, Bin Yu, M. Vetterli, *IEEE Trans. Image Process.*, **9**, No. 9, 1532–1546 (2000), doi: 10.1109/83.862633.
37. M. Srivastava, C. L. Anderson, J. H. Freed, *IEEE Access*, **4**, 3862–3877 (2016), doi: 10.1109/ACCESS.2016.2587581.
38. Z. Wang, A. C. Bovik, H. R. Sheikh, E. P. Simoncelli, *IEEE Trans. Image Process.*, **13**, No. 4, 600–612 (2004), doi: 10.1109/TIP.2003.819861.
39. I. W. Selesnick, *IEEE Trans. Signal Process.*, **52**, No. 5, 1304–1314 (2004), doi: 10.1109/TSP.2004.826174.
40. T. S. Sharan, S. Sharma, N. Sharma, *J Appl. Spectr*., **88**, 117–124 (2021), doi: 10.1007/s10812-021-01149-9.